

Flow Immediately behind a Step in a Simulated Supersonic Combustor

R. C. Orth* and J. M. Cameron†
The Johns Hopkins University, Silver Spring, Md.

Results are presented from a series of nonburning flow tests in which extensive instream and wall pressure and fluid sample measurements were made to characterize the flow immediately behind a rearward facing step in a simulated supersonic combustor. Pitot pressure data were used to determine simplified flowfield models for the cases of flow both with and without a simulated precombustion shock and simulated fuel injection. The effects of the shock on the flowfield and fuel-air distribution in the main stream and recirculation zone behind the step, as well as the implications for the placement of ignition devices and piloting, are discussed.

Introduction

IN supersonic combustion ramjet (scramjets), certain combustor configurations employ in their design a rearward facing step downstream of the fuel injector. This sudden step increase in combustor area has been beneficial to combustor operation in several ways. Among these are: 1) the step helps to isolate or limit the interaction of the combustion process with the inlet flowfield of the engine; 2) the step limits the combustor pressure rise by spreading the pressure gradient from the combustion shock along the wall, limiting excessive local heat transfer due to shock impingement; and 3) the step serves as a flame-holding region. The purpose of the present work is to improve the understanding of the flow patterns and fuel distribution in the mainstream and in the recirculation zone behind the step, so that fuel injectors and/or ignition aids can be located more effectively to improve the supersonic combustion of hydrocarbon fuels or fuel blends.

Generally, in supersonic combustion, an oblique shock will be present at the combustor entrance. Waltrup and Billig developed a semi-empirical pseudo-one-dimensional analysis that defined the pressure field and attendant separation zone in the precombustion interaction region of constant area combustors.¹⁻³ Waltrup and Cameron presented wall shear and boundary-layer measurements that completed the depiction of the instream and wall flow structure for a shock-separated flow of this type.⁴ These works also demonstrated the feasibility of producing the shock structure and shock/boundary-layer interactions analogous to those present at the combustor entrance in a simple nonreacting system, where throttling rather than combustion is the cause of compression. This technique permits detailed measurement of the flowfield to be made in a much less hostile environment where instrumentation will not be destroyed by the high temperatures ($\sim 4000^\circ\text{R}$ - 5000°R) encountered in flows with combustion. Although exact duplication of local flow divergence caused by spatial and time variations in heat release cannot be achieved with throttling, extensive comparison of the throttle test data and combustor data showed that sufficient similarity of the two flows was obtained for studying the effects of the com-

bustion shock structure on boundary-layer separation, wall interaction and fuel penetration and spreading.

This paper describes the extension of the previous work using throttling to simulate combustion shocks to the case where a rearward facing step is present downstream of the combustion shock. The pressure data and analysis reported herein show the effects of the interaction of the step and the simulated combustion shock on the instream flow structure and the recirculation zone.

Since many of the liquid fuels under consideration for use in scramjets are toxic, as well as pyrophoric, liquid Freon was used to simulate the fuel in the present tests. In the region of interest, i.e., just behind the step, the Freon and the fuel in a scramjet are undergoing a phase change from liquid to gas. The two-phase flow makes precise determination of the fuel-air mixture at any point extremely difficult. However, previous studies of liquid injection into supersonic streams^{5,6} have shown that penetration and spreading can be readily related to jet-freestream momentum ratio. Furthermore, even though exact mass balances may not be achieved, fluid sampling in the two-phase flow can be used to delineate the injectant edges and core regions quite accurately. Thus, the gas sample data in the present work provide a qualitative picture of the fuel distribution just downstream from the step and in the recirculation zone where fuel ignition devices are likely to provide maximum increases in engine performance.

Experimental Apparatus and Test Procedure

Figure 1 is a schematic of the experimental setup used to simulate the flow in a supersonic combustion step combustor. In each test, compressed air (~ 80 psia, $\sim 520^\circ\text{R}$) was expanded through a contoured axisymmetric nozzle into an isolation section, then through a fuel-injector-step section, a recirculation zone section, a simulated combustor section, and then exhausted through a hydraulically-operated ball valve to atmosphere or a vacuum. Wall pressures were monitored through 0.015-in.-diameter holes drilled 1 in. apart in the isolator and combustor sections and 0.25 in. apart in the recirculation zone section. The recirculation zone test section is made up of 0.5-in.-thick washers.

A 9-point cruciform rake, designed to replace the fuel injector, and a 23-point bar rake, designed to replace one of the recirculation zone test section washers, were used to make instream pressure surveys upstream and downstream of the step, respectively. The pitot probes on both rakes are spaced to monitor equal annular areas and the duct centerline. To minimize possible interference, the pitot probes from adjacent annular flow areas were alternated on different arms of the rakes. In the recirculation zone, the four outer probes on each

Submitted October 17, 1974; presented at AIAA/SAE 10th Propulsion Conference, San Diego, California, October 21-24, 1974; revision received January 24, 1975. This work was supported by the United States Navy under Naval Ordnance Systems Command Contract N00017-72-C-4401.

Index categories: Shock Waves and Detonations; Airbreathing Propulsion; Boundary Layers and Convective Heat Transfer—Turbulent.

*Senior Engineer, Propulsion Group, Applied Physics Laboratory. Member AIAA.

†Engineer Staff Associate, Propulsion Group, Applied Physics Laboratory.

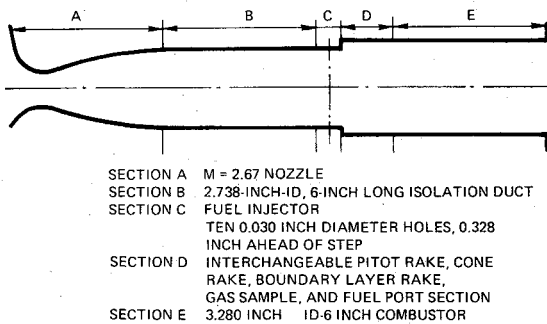


Fig. 1 Step combustor recirculation zone test configuration.

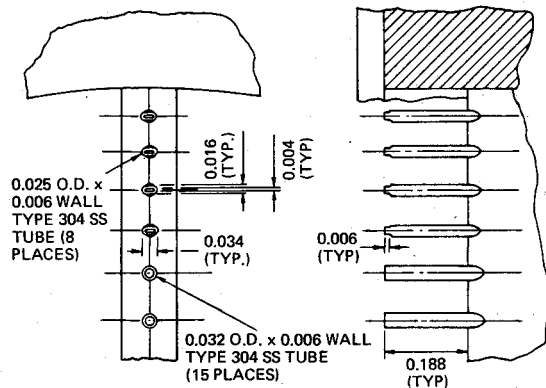


Fig. 2 Bar rake detail.

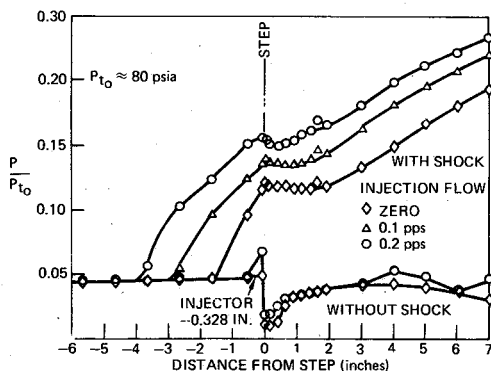


Fig. 3 Wall static pressure distribution in recirculation zone test.

side of the bar rake were flattened boundary-layer probes of smaller diameter as shown in Fig. 2. All pressures were measured by strain-gage transducers calibrated within $\pm 0.5\%$ of their full-scale value, 50 psia for the pitot probes and 25 psia for the wall static ports. The transducers were mounted in a scanning valve arrangement, operating at 16 pressure samples per second.

Two conditions were run during each test, with and without a simulated combustion shock. To generate the wave structure simulating the combustion shock, air flow was first established in the test section. Then the ball valve was partially closed, throttling the flow and forcing a series of oblique waves to proceed upstream into the test section. By monitoring the wall pressures, the first (strongest) wave was positioned at the same point in the test section for each test. For the second part of the test, the valve was moved to the full open position and the air flow was exhausted through a vacuum system.

To simulate fuel injection, Freon 122 (dichlorodifluoromethane) was injected through ten 0.030-in.-diam fuel ports at a mass flow rate of about 0.22 lb/sec, simulating an overall fuel-air equivalence ratio of 0.8 for a typical high-energy liquid fuel with the air mass flow of 3.3 lb/sec. Instream fluid samples within the first 2 in. behind the

step were obtained using the 23-point bar rake described above. In successive tests, these measurements and pitot pressure measurements were made in three different radial planes: directly behind one Freon jet, one-quarter of the way between two jets, and half-way between two jets. Fluid samples were also taken through sample ports in the duct wall. The samples were analyzed on a combustion gas analysis system.⁷ This is a specially designed gas chromatograph that features precise carrier gas controls, sample handling and pressure measurement techniques. Samples are typically analyzed to an accuracy within $\pm 0.5\%$.

Test Results and Data Analysis

Pressure Data

Wall pressure profiles for the cases of no Freon injection and Freon injection, both with and without the simulated combustion shock are shown in Fig. 3. For comparison profiles from an actual combustion test are shown in Fig. 3. For comparison profiles for an actual combustion test are shown in Fig. 4. The wall pressure profiles for the shock-free recirculation zone test (Fig. 3) are similar in shape to that of the cold point (no fuel flow) for the combustor test (Fig. 4). These profiles show a sharp decrease in pressure caused by separation of the flow as it crosses the step, a rise in pressure as the flow reattaches 1 to 2 in. downstream, and a slow decline 4 to 8 in. downstream as the reflected expansion waves from the step strike the duct walls. Because of the difference in Mach number between the two tests, i.e., 2.65 in these tests vs. 3.23 in the combustion tests, the distances at which the various events occur do not correspond precisely.

For the shock-free case, mass injection raises the wall static pressure slightly around the injection ports and in the recirculation zone behind the step. With a simulated combustion shock, mass injection significantly raises the level of the wall static pressure at all stations. The larger separated regions (discussed in detail, below) created by the shock-step interaction permit extensive transmittal of the mass-injection-induced wall pressure disturbances throughout the simulated combustion shock region. The effect is to move the entire wave system upstream. To facilitate data comparison, the simulated shock location for the mass injection cases was positioned (by throttling) in the same location as the simulated shock cases without injection.

Pitot pressure profiles behind the centerline of one fuel port are shown for the cases of no shock with no injection, simulated shock with no injection, no shock with mass injection and simulated shock with mass injection in Figs. 5a, 5b, 6a, and 6b, respectively. Data without the shock present are typical for supersonic flow over a rearward facing step⁸ and show the well-defined recirculation zone directly behind the step and the pressure rise associated with the lip shock and reattachment shock. Note that the value of the pitot pressure measured at 0.125 in behind the step, in the recirculation zone, Fig. 5a, is roughly three times the value of the wall static

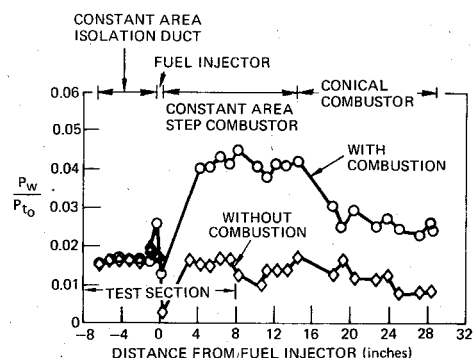


Fig. 4 Combustor wall static pressure distribution in step-cyl-cone combustor with and without combustion.

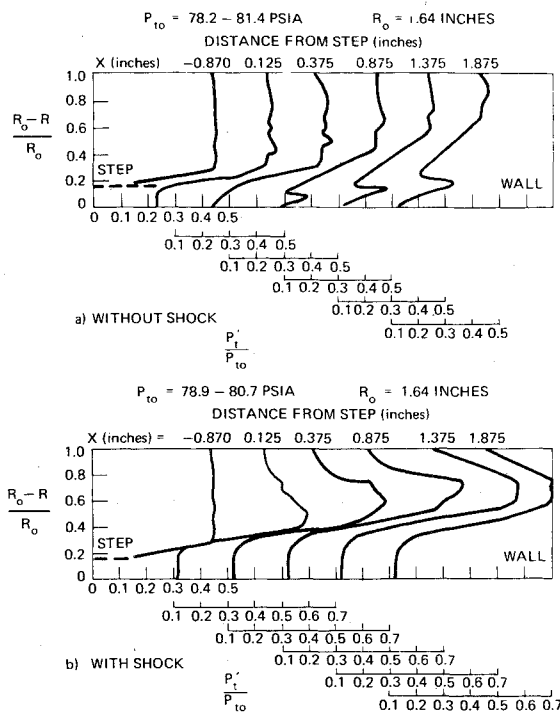


Fig. 5 Pitot pressure with and without simulated combustion shock.

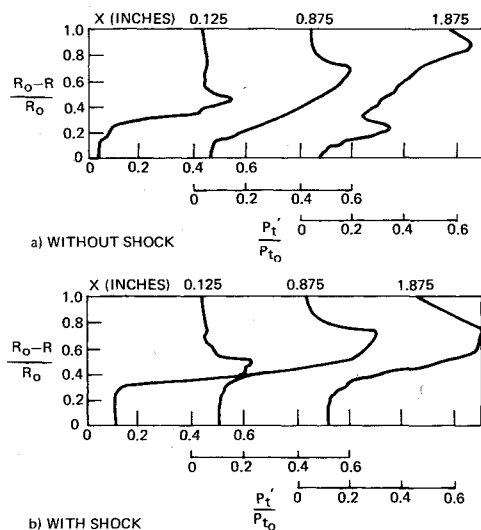


Fig. 6 Pitot pressure— C_L fuel port with and without shock with fuel.

pressure measured on the step face and the duct wall in that region, Fig. 3 ($P_t/P_{t0} \approx 0.03$ vs $P/P_{t0} \approx 0.01$). The support arrangement prohibited simultaneous pitot and wall-static measurements in that region with the rake in the 0.125 in. position. However, a wall pressure profile measured in a plane not aligned with the rake and with the rake located 0.375 in. behind the step was almost identical with that when the rake was not present indicating little or no probe interference. It appears that the pitot rake caused local disturbance of the recirculation zone, i.e., at 0.125 in. behind the step, making detailed flow analysis impossible in that region. Outside the recirculation zone, no such interference was encountered.

In the entire distance (1.875 in.) downstream from the step where measurements were made, the profiles with the simulated shock present (Fig. 5b) show a uniform, low-pressure, separated recirculation zone near the wall extending well above the height of the step. In this enlarged recirculation zone the pitot pressure is approximately equal to the wall static pressure. However, because the pressure differences

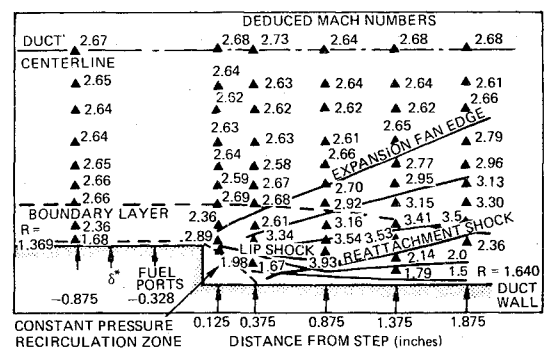


Fig. 7 Constant Mach number profiles for Mach 2.67 flow over a step deduced from pitot pressure profiles.

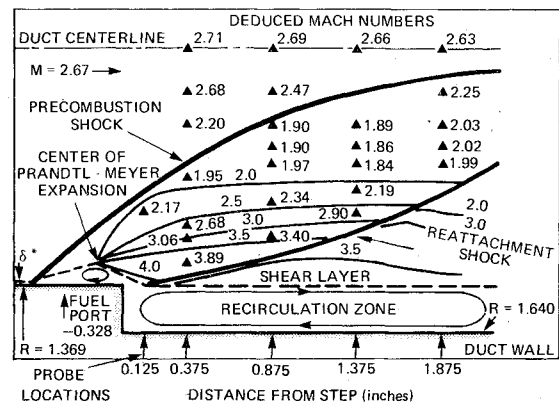


Fig. 8 Constant Mach number profiles with a simulated precombustion shock but without Freon injection deduced from pitot pressure profiles.

were so small and the pressure levels were at the low end of the transducer range (6 psia out of 50 psia), detailed analysis of the flowfield in the recirculation zone was not attempted. Except for small local perturbations, the pitot pressure data with Freon injection both without and with the simulated shock (Fig. 6) are similar to those without injection (Fig. 5).

Flowfield Models

Simplified flowfield models and Mach number profiles for the shock-free and simulated combustion shock without injection have been developed from extensive analyses of the pitot and wall pressure data. For the shock-free no-injection case, Fig. 7, the relationship between the measured pitot pressure and known tunnel total pressure was used to compute local Mach number directly from the pitot pressure Mach function. At the station 0.875 in. upstream from the step the static pressure through the boundary layer was assumed to be equal to the measured wall static pressure. The Mach number, and consequently the total pressure loss, at each point was determined from the Rayleigh pitot formula. By tracking streamlines through the Prandtl-Meyer expansion over the step, total pressure and Mach number were determined at each point of pitot pressure measurement.

Lip shock angle and reattachment shock angle were determined graphically from the pitot-pressure data. Appropriate two-dimensional, two-shock, and three-shock models (an oblique shock and normal probe shock, or two-oblique shocks and a probe shock) were used in the regions downstream of the lip shock and reattachment shock. The two-dimensional models are only strictly applicable near the duct wall and above the viscous boundary-layer region where the effects of curvature are small. Nevertheless, by using the measured pitot pressures and adjusted total pressure as described above, and by making local adjustments in the model (flow direction turning angle, etc.), a reasonably good definition of the flow

was developed. Of interest are the points of deduced Mach numbers ~ 2.60 in Fig. 7 which project back to a point on the wall where tunnel sections B and C joined together unevenly and generated a weak shock wave.

In modeling the flowfield for the simulated combustion-shock case (Fig. 8), the position of the simulated precombustion shock was determined from the locations of the maximum values in pitot pressure data at each station behind the step. The shock angle was determined by extending the shock line back to the point of flow separation as determined from the duct wall pressure data. The two-dimensional wedge flow turning angle required to support this precombustion shock angle gave the estimated boundary-layer-separation zone. The top of the separated zone, the point of location for the centered Prandtl-Meyer expansion, was determined by the intersection of the separation line with the Mach line for flow behind the precombustion shock that went through the point where bending of the shock first occurred. The shear layer behind the step was positioned at the top of the low-pressure, constant-pressure region on the measured pitot profiles. The location of the reattachment shock and the shock angle were determined by iteration of the Mach number ahead of reattachment and the required turning angle to give axial flow downstream of reattachment. With these flow features identified, the detailed Mach number contours were determined by solution of the normal shock model (upstream of the precombustion shock), the two-shock model (between precombustion and reattachment shocks), or the three-shock model (downstream from the reattachment shock) at each pitot-pressure measurement point.

In Fig. 8, the large recirculation zone behind the step is shown extending downstream beyond 2 in. behind the step. Since pitot measurements were not made beyond this point the exact extent of the recirculation zone for simulated combustion is unknown. However, from comparison of the wall pressure data in Figs. 3 and 4, one can see that the flow in both the simulated combustion and actual combustion cases reattaches to the wall between 2 and 4 in. downstream from the step. Thus, even though streamline divergence and regions of low mass flux due to supersonic combustion have not been exactly duplicated, the basic flow features, particularly in the region of the fuel injector and step, have been more than adequately simulated by the throttling process.

Modeling of the combustor flowfield is complicated by the fact that the shock structure is a family of finite compressions rather than idealized planar waves (Ref. 3). The result of this is a variation in the Mach number determined from pitot probe measurements when moving from the duct centerline in the undisturbed flow toward the position of the simulated precombustion shock. This variation is different from that which occurs downstream of the precombustion shock, where the three-dimensional effects of the axisymmetric duct flow cause the constant-Mach-number lines in the expansion fan from the step and behind the reattachment shock to be bent over parallel to the duct centerline. Without these effects, the constant-Mach-number lines would follow two-dimensional expansion waves as straight lines from the centered Prandtl-Meyer expansion until they intersected the precombustion shock, causing it to bend downstream. The shock is still bent downstream but not as much as in the two-dimensional case. In addition, the effect of the step is greatly reduced near the duct centerline, as seen by the region of relatively constant Mach number between the simulated precombustion shock and the Mach 2 contour.

To aid in the analysis of the gas sample data, discussed below, air mass flux profiles were computed from the pitot pressure and Mach number profiles. For the simulated-combustion shock case at the station 0.125 in. downstream from the step an air mass flow of 3.1 pps was computed between the duct centerline and the separated zone. Total measured air flow was 3.3 pps, indicating ~ 0.2 pps of air flowing through the recirculation zone. These values appear reasonable and support the simplified flow model. At the

0.875 in. downstream station, the computed mass flow within the main stream was 3.5 pps with excessively high mass flux values occurring between the simulated shock and the Mach 2.0 profile shown in Fig. 8. As discussed earlier, this is a region of strong three-dimensional flow where the inaccuracies of two-dimensional modeling lead to sizable errors in mass flux computation. Reduction of the computed mass-flux in this region by 15% led to a balance between the computed and measured mass flow rate.

Fluid Sample Data

Measured Freon concentration profiles without and with the simulated combustion shock (Fig. 9) show that the shock significantly alters the injectant penetration and distribution just behind the step. Without the shock (Fig. 9a) the injectant is swept around the corner by the expanding flowfield, creating a relatively thin, poorly mixed, high-Freon-concentration ring around the duct wall. In tests of single liquid jets normal to a flat plate, Kush and Schetz⁵ discovered that a layer of liquid was stripped off the jet and swept down the surface of the plate. Apparently the same phenomenon is occurring here in the shock-free case, and the liquid layer is swept around the corner and into the recirculation zone. Such a high fuel concentration would be well beyond the corresponding rich ignition limit. With the shock present (Fig. 9b), the Freon penetrates farther into the supersonic crossflow. Furthermore, good mixing occurs downstream of this shock, so that the Freon-air distribution 1.875 in. from the step is almost uniform with a maximum value of 8%.

From cross-plots of the above profiles and data taken one-quarter and one-half the way between ports, circumferential variations of injectant concentration were determined. Plots for two downstream locations for the shock-free and shock case are shown in Figs. 10 and 11. For fuel ignition considerations, the shock-free case is the primary one of interest. Wall sample data taken 0.125 in. (Fig. 10a) behind the step show an almost uniform layer of pure Freon on the duct wall just behind the step. As the flow proceeds downstream, the Freon vaporizes and mixes with the recirculating air along the wall. Because of the expanding supersonic flow in the main-stream, the Freon jets are swept down close to the wall, so that the injectant concentration remains quite high in the recirculation zone ahead of flow reattachment, which occurs

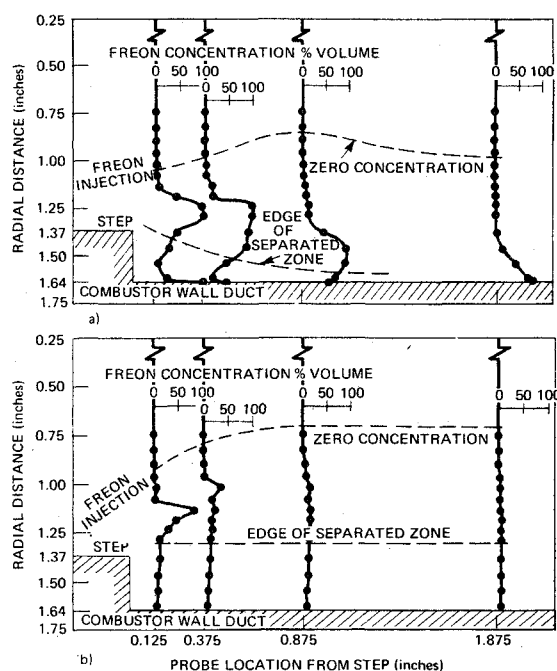


Fig. 9 Measured Freon-air concentrations directly behind one injector port: a) without a simulated combustion shock; b) with a simulated combustion shock.

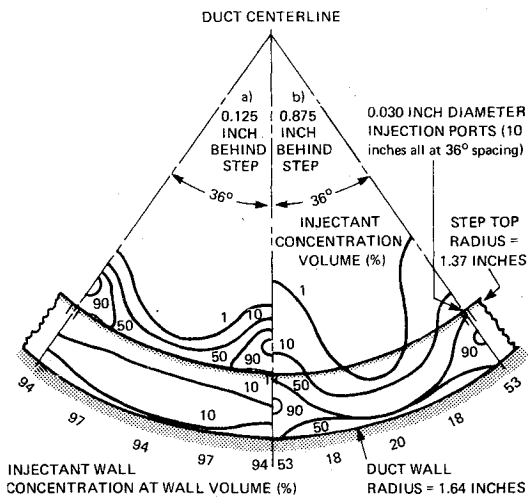


Fig. 10 Circumferential variation in Freon-122 injectant concentration deduced from gas sample measurements at: a) 0.125 in. behind step; and b) 0.875 in. behind step, without simulated precombustion shock.

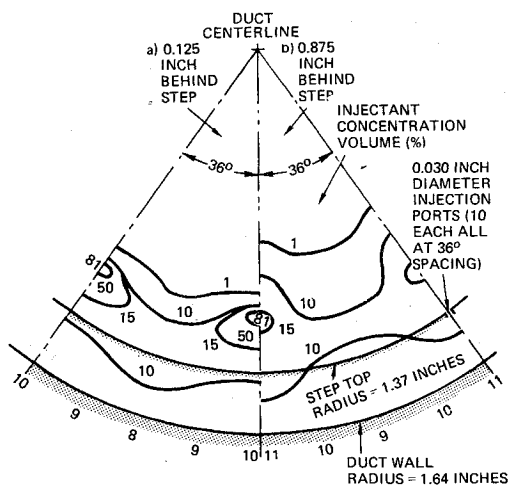


Fig. 11 Circumferential variation in Freon-122 injectant concentration deduced from gas sample measurements at: a) 0.125 in. behind step; and b) 0.875 in. behind step, with simulated combustion shock.

about 1.375 in. downstream from the step. The circumferential variations for the shock case (Fig. 10b) show how the shock mixes the Freon circumferentially as well as radially. At both downstream locations the Freon penetration between ports is nearly equal to that behind the ports. The concentration at the wall is almost identical to the instream concentration and shows no evidence of the presence of a liquid layer on the wall surface. The large separation region at the top of the step allows the injectant to penetrate out into the stream behind the step without shedding, where the shock-induced higher mixing rates yield more uniform concentrations.

The overall Freon-air flow rates were chosen so as to correspond to typical fuel-air flow rates used in the direct-connect supersonic combustor tests. With these rates, complete mixing of the injectant airstream in the present tests would yield a volumetric injectant concentration of 1.5%, simulating $ER \approx 0.8$. Complete mixing with the air bounded by the zero injectant concentration boundary in the recirculation zone would yield average volumetric concentrations of 2.2 and 2.6% for the shock and shock-free cases, respectively. To put it another way, roughly 30% to 40% of the air flow past this station is in a central core region not yet reached by the Freon. There are several complicating factors which

must be accounted for to compute the local "fuel"-air mass ratios. Yates⁶ has given detailed discussion of the problems of mass flux sampling in the two-phase flow that exists just behind the injector and step. Beside the local variation in air mass flux, which was discussed earlier, the problems of probe performance and injectant phase identification still remain. Mass flux computations were made in which the injectant was considered to remain in the liquid phase within the probe. The resulting computed mass injectant rate was several times the actual measured Freon flow into the injector. Proper definition of the injectant phase at the probe tip would alter the computed mass flux values somewhat, but not enough to account for so large a difference. The large error in the mass sampling measurements arose from using pitot probes as sampling probes and was anticipated before the experiments were initiated. The standoff shock associated with the pitot probe causes the flow to deviate ahead of the probe. The heavier Freon molecules tend to deviate less, and therefore, measured concentration is increased. Furthermore, intermittent drops of liquid Freon tended to block the small diameter probes, which have no internal expansion (which would aid vaporization). This further increased the injectant mass in the probe leading to the overly rich injectant concentrations. Because a large number of probes were necessary to document the flow, this precluded the use of larger (than pitot probes) gas sample probes designed to keep the normal shock attached and with a large internal expansion. Qualitative rather than quantitative measurements were felt to be sufficient for the present set of tests.

Even though the sampling data led to excessively large injectant mass flows the data are still useful for qualitatively defining the extreme regions of the injectant penetration and spreading. At very rich and very lean concentrations, the probe-induced errors are relatively smaller. Thus, the measured concentration contour can still be used to locate the injectant-rich and lean regions of the flow behind the step with and without the simulated-precombustion shock.

Conclusions and Application of Supersonic Combustion Testing

From this extensive set of pressure and fluid sample measurements behind a step in an axisymmetric duct, the following conclusions are drawn. 1) Simulated combustion shocks similar to those in a supersonic step combustor can be readily generated by controlling the back pressure in the duct by means of a butterfly valve at the duct exit. 2) Good descriptions of the flowfield both with and without the simulated shock and Freon injection (to simulate fuel injection) were determined from the measurements. 3) The combustion shock dramatically alters the flowfield behind the step, reduces the liquid layer on the wall surface behind the step and enhances injectant-air mixing at that region.

Finally, the tests have provided considerable insight into the fuel-air mixing phenomena associated with ignition and combustion in supersonic combustors. In the shock-free case, which is the one of interest for fuel ignition, the tests show that the fuel-air mixture in the recirculation zone behind a step in a supersonic combustor is likely to be exceedingly fuel rich. Also ignition devices should be placed between fuel injection ports, near the point of shock reattachment where the fuel-air mixture is more likely to be near stoichiometric, or at least less than the fuel rich ignition limit. The fuel-rich mixtures in the recirculation zone also suggest placement of oxygen pilots in that region to provide the free oxygen required by these ignition devices.

References

- Billig, F. S., Dugger, G. L., and Waltrup, P. J., "Inlet-Combustor Interface Problems in Scramjet Engines," *1st International Symposium on Air Breathing Engines*, The International Airbreathing Propulsion Committee, Marseilles, France, June 1972.

²Waltrup, P. J. and Billig, F. S., "Prediction of Precombustion Wall Pressure Distributions in Scramjet Engines," *Journal of Spacecraft and Rockets*, Vol. 10, Sept. 1973, pp. 620-622.

³Waltrup, P. J. and Billig, F. S., "The Structure of Shock Waves in Cylindrical Ducts," *AIAA Journal*, Vol. 11, Oct. 1973, pp. 1404-1408.

⁴Waltrup, P.J. and Cameron, J.M., "Wall Shear and Boundary-Layer Measurements in Shock Separated Flow," *AIAA Journal*, Vol. 12, June 1974, pp. 878-880.

⁵Kush, E. A., Jr. and Schetz, J. A., "Liquid Jet Injection into a

Supersonic Flow," *AIAA Journal*, Vol. 11, Sept. 1973, pp. 1223-1224.

⁶Yates, C.L., "Liquid Injection into a Supersonic Stream," Tech. Rept. AFAPL-TR-71-97, Vol. 1, March 1972, Air Force Aero Propulsion Laboratory, Wright-Patterson AFB, Ohio.

⁷Orth, R. C., "Gas Chromatography for Combustion Gas Analysis," *APL Technical Digest*, Vol. 12, July-Sept. 1973, pp. 2-10.

⁸Sherberg, M. G. and Smith, H. E., "An Experimental Study of Supersonic Flow Over a Rearward Facing Step," *AIAA Journal*, Vol. 5, Jan. 1967, pp. 51-56.

From the AIAA Progress in Astronautics and Aeronautics Series . . .

INSTRUMENTATION FOR AIRBREATHING PROPULSION—v. 34

*Edited by Allen Fuhns, Naval Postgraduate School, and
Marshall Kingery, Arnold Engineering Development Center*

This volume presents thirty-nine studies in advanced instrumentation for turbojet engines, covering measurement and monitoring of internal inlet flow, compressor internal aerodynamics, turbojet, ramjet, and composite combustors, turbines, propulsion controls, and engine condition monitoring. Includes applications of techniques of holography, laser velocimetry, Baman scattering, fluorescence, and ultrasonics, in addition to refinements of existing techniques.

Both inflight and research instrumentation requirements are considered in evaluating what to measure and how to measure it. Critical new parameters for engine controls must be measured with improved instrumentation. Inlet flow monitoring covers transducers, test requirements, dynamic distortion, and advanced instrumentation applications. Compressor studies examine both basic phenomena and dynamic flow, with special monitoring parameters.

Combustor applications review the state-of-the-art, proposing flowfield diagnosis and holography to monitor jets, nozzles, droplets, sprays, and particle combustion. Turbine monitoring, propulsion control sensing and pyrometry, and total engine condition monitoring, with cost factors, conclude the coverage.

547 pp. 6 x 9, illus. \$14.00 Mem. \$20.00 List

TO ORDER WRITE: Publications Dept., AIAA, 1290 Avenue of the Americas, New York, N. Y. 10019